

CRYSTALLINE EVOLUTIONS IN CHESSBOARD-LIKE MICROSTRUCTURES

ANNALISA MALUSA[†] AND MATTEO NOVAGA[‡]

ABSTRACT. We describe the macroscopic behavior of evolutions by crystalline curvature of planar sets in a chessboard-like medium, modeled by a periodic forcing term. We show that the underlying microstructure may produce both pinning and confinement effects on the geometric motion.

CONTENTS

1. Introduction	1
Acknowledgments.	3
2. Setting of the problem	3
Notation	3
The crystalline curvature	3
Forced crystalline flows	4
3. Calibrability conditions	5
4. Forced crystalline flows and their effective motion	9
References	21

1. INTRODUCTION

We are concerned with the asymptotic behavior of motions of planar curves according to the law

$$(1) \quad v = \kappa + g\left(\frac{x}{\varepsilon}, \frac{y}{\varepsilon}\right),$$

where v is the normal velocity, κ is the crystalline curvature, $g : \mathbb{R}^2 \rightarrow \mathbb{R}$ is a periodic forcing term, with average \bar{g} , and $\varepsilon > 0$ is a small parameter which takes account of the frequency of oscillation.

Date: November 18, 2018.

2010 Mathematics Subject Classification. Primary 53C44, Secondary 35B27.

Key words and phrases. Crystalline flow, homogenization, facet-breaking, pinning.

[†] Dipartimento di Matematica “G. Castelnuovo”, Sapienza Università di Roma, Piazzale Aldo Moro 2, 00185 Roma, Italy, email: malusa@mat.uniroma1.it.

[‡] Dipartimento di Matematica, Università di Pisa, Largo B. Pontecorvo 5, 56217 Pisa, Italy, email: matteo.novaga@unipi.it.

Crystalline evolutions provide simplified models for describing several phenomena in Materials Science (see [24, 26, 27] and references therein) and have been significantly studied in recent years (see for instance [1, 21, 3, 4, 16, 17, 18, 20]).

The forcing term g models a rapidly oscillating heterogeneous medium and, in the homogenization limit $\varepsilon \rightarrow 0$, the oscillations of the medium affect the velocity of the evolving front. The geometric motion (1) corresponds to the gradient flow of the energy

$$F_\varepsilon(E) = \int_{\partial E} (|\nu_1^E| + |\nu_2^E|) d\mathcal{H}^1 + \int_E g\left(\frac{x}{\varepsilon}, \frac{y}{\varepsilon}\right) d\mathcal{L}^2, \quad E \subset \mathbb{R}^2,$$

where we identify the evolving curve with the boundary of a set E . Since the volume term converges to $\bar{g} \mathcal{L}^2(E)$ as $\varepsilon \rightarrow 0$, the Γ -limit of the functionals F_ε (see [6]) is given by

$$\bar{F}(E) = \int_{\partial E} (|\nu_1^E| + |\nu_2^E|) d\mathcal{H}^1 + \bar{g} \mathcal{L}^2(E).$$

Hence, our analysis can be set in a large class of variational evolution problems dealing with limits of motions driven by functionals F_ε depending on a small parameter.

For oscillating functionals like F_ε , the energy landscape of the energies can be quite different from that of their Γ -limit, and the related motions can be influenced by the presence of local minima which may give rise to pinning phenomena, or to effective homogenized velocities (see [25, 2, 9, 7]). In the case of geometric motions, a general understanding of the effects of microstructure is still missing. Recently, some results have been obtained for two-dimensional crystalline energies, for which a simpler description can be given in terms of a system of ODEs (see for instance [9, 11, 8, 12, 9, 10]).

Coming back to our specific problem (1), we assume for simplicity that g takes only two values $\alpha < 0 < \beta$, its periodicity cell is $[0, 1]^2$, and that $\bar{g} = \frac{\alpha + \beta}{2}$. We also assume that g has a chessboard structure, as specified in (2) below.

After a careful analysis, it turns out that curves evolving by (1) undergo a microscopic “facet-breaking” phenomenon at a scale ε , with small segments of length proportional to ε being created and, in some cases, subsequently reabsorbed. The macroscopic effect of this behavior is a “pinning effect” for the limit evolution, corresponding to the possible onset of new edges, with slope of 45 degrees and zero velocity (depending on the initial set and on the values α, β). On the other hand, the horizontal and the vertical edges always travel with the asymptotic velocity $\kappa + \bar{g}$. We thus obtain a characterization of the limit evolution, which is the main result of this paper, and is stated precisely in Theorems 4.7 and 4.8.

We point out that, due to the possible presence of these new edges with zero velocity, the limit flow does not coincide with the gradient flow of the limit functional \bar{F} , which is simply given by $v = \kappa + \bar{g}$.

We recall that, in a previous paper [10], we considered a similar homogenization problem where the periodic function g depends only on the horizontal variable, so that the medium has a stratified, opposite to a chessboard-like, structure.

It would be very interesting to extend our analysis to the isotropic variant of (1), where the crystalline curvature κ is replaced by the usual curvature of the evolving curve, so that (1) becomes a forced curvature flow. However, as such evolution cannot be described in terms of a system of ODEs, different techniques would be needed (partial results in this direction can be found in [15, 14]).

The plan of the paper is the following: in Section 2 we introduce the notion of crystalline curvature and the evolution problem we are interested in. In Section 3 we introduce the notion of calibrable edge, that is, an edge which does not break during the evolution, and we state the calibrability conditions. Finally, in Section 4 we characterize explicitly the limit evolution as $\varepsilon \rightarrow 0$, for initial data which are squares (Theorem 4.7) and more generally rectangles (Theorem 4.8).

Acknowledgments. The authors wish to thank Andrea Braides for useful discussions on the topic of this paper. The second author was partially supported by the Italian CNR-GNAMPA and by the University of Pisa via grant PRA-2017 “Problemi di ottimizzazione e di evoluzione in ambito variazionale”.

2. SETTING OF THE PROBLEM

Notation. The canonical basis of \mathbb{R}^2 will be denoted by $e_1 = (1, 0)$, $e_2 = (0, 1)$.

The 1-dimensional Hausdorff measure and the 2-dimensional Lebesgue measure in \mathbb{R}^2 will be denoted by \mathcal{H}^1 and \mathcal{L}^2 , respectively.

We say that a set $E \subseteq \mathbb{R}^2$ is a *Lipschitz set* if its boundary ∂E can be written, locally, as the graph of a Lipschitz function (with respect to a suitable orthogonal coordinate system). The *outward normal* to ∂E at ξ , that exists \mathcal{H}^1 -almost everywhere on ∂E , will be denoted by $\nu^E = (\nu_1^E, \nu_2^E)$.

The Hausdorff distance between two sets $E, F \in \mathbb{R}^2$ will be denoted by $d_H(E, F)$.

The crystalline curvature. We briefly recall a notion of curvature κ^E on ∂E which is consistent with the requirement that a geometric evolution $E(t)$, reducing as fast as possible the energy

$$P_\varphi(E) := \int_{\partial E} (|\nu_1^E| + |\nu_2^E|) d\mathcal{H}^1,$$

has normal velocity $\kappa^{E(t)}$ \mathcal{H}^1 -almost everywhere on $\partial E(t)$.

The surface tension $\varphi^\circ(x, y) = |x| + |y|$ is the polar function of the convex norm $\varphi(x, y) = \max\{|x|, |y|\}$, $(x, y) \in \mathbb{R}^2$, so that $P_\varphi(E)$ turns out to be the perimeter associated to the anisotropy $\varphi(x, y)$, that is, the Minkowski content obtained by considering (\mathbb{R}^2, φ) as a normed space. The sets $\{\phi(\xi) \leq 1\}$ and $\{\phi^\circ(\xi) \leq 1\}$ are the square $K = [-1, 1]^2$, and the square with corners at $(\pm 1, 0)$ and $(0, \pm 1)$, respectively.

Given a nonempty compact set $E \subseteq \mathbb{R}^2$, if we denote by d^E the *oriented φ -distance function* to ∂E , negative inside E , that is,

$$d^E(\xi) := \inf_{\eta \in E} \varphi(\xi - \eta) - \inf_{\eta \notin E} \varphi(\xi - \eta), \quad \xi \in \mathbb{R}^2.$$

The normal cone at $\xi \in \partial E$ is well defined whenever ξ is a differentiability point for d^E , and it is given by $T_{\varphi^\circ}(\nabla d^E(\xi))$, where

$$T_{\varphi^\circ}(\xi^\circ) := \{\xi \in \mathbb{R}^2, \xi \cdot \xi^\circ = (\varphi^\circ(\xi))^2\}, \quad \xi^\circ \in \mathbb{R}^2.$$

The notion of intrinsic curvature in (\mathbb{R}^2, φ) is based on the existence of regular selections of $T_{\varphi^\circ}(\nabla d^E)$ on ∂E .

Definition 2.1 (φ -regular set, Cahn–Hoffmann field, φ -curvature). We say that a set $E \subseteq \mathbb{R}^2$ is φ -regular if ∂E is a compact Lipschitz curve, and there exists a vector field $n_\varphi \in \text{Lip}(\partial E; \mathbb{R}^2)$ such that $n_\varphi \in T_{\varphi^\circ}(\nabla d^E)$ \mathcal{H}^1 -almost everywhere in ∂E . Any selection of the multivalued function $T_{\varphi^\circ}(\nabla d^E)$ on ∂E is called a *Cahn–Hoffmann vector field* for ∂E , and $\kappa = \text{div } n_\varphi$ is the related φ -curvature (or *crystalline curvature*) of ∂E .

Remark 2.2 (Edges and vertices). A direct computation gives that $T_{\varphi^\circ}(\xi^\circ)$ is a singleton if $\varphi^\circ(\xi^\circ) = 1$, and ξ° is not a coordinate vector. Moreover one gets

$$\begin{cases} T_{\varphi^\circ}(e_1) &= \llbracket (1, 1), (1, -1) \rrbracket, \\ T_{\varphi^\circ}(e_2) &= \llbracket (-1, 1), (1, 1) \rrbracket, \\ T_{\varphi^\circ}(-e_1) &= \llbracket (-1, 1), (-1, -1) \rrbracket, \\ T_{\varphi^\circ}(-e_2) &= \llbracket (-1, -1), (1, -1) \rrbracket. \end{cases}$$

(Here and in the following $\llbracket \xi, \eta \rrbracket$ is the closed segment joining the vector ξ with η). The boundary of a φ -regular set E is given by a finite number of maximal closed arcs with the property that $T_{\varphi^\circ}(\nabla d^E)$ is a fixed set T_A in the interior of each arc A . This set T_A is either a singleton, if the arc A is not a horizontal or vertical segment, or one of the closed convex cones described above. The maximal arcs of ∂E which are straight horizontal or vertical segments will be called *edges*, and the endpoints of every arc will be called *vertices* of ∂E .

The requirement of Lipschitz continuity keeps the value of every Cahn–Hoffmann vector field fixed at vertices. Hence, in order to exhibit a Cahn–Hoffmann vector field n_φ on ∂E it is enough to construct a field $n_A \in \text{Lip}(A; \mathbb{R}^2)$ on each arc A , with the correct values at the vertices, and satisfying the constraint $n_A \in T_A$. In what follows, with a little abuse of notation, we shall call n_A the Cahn–Hoffmann vector field on the arc A .

Forced crystalline flows. Let $\alpha < 0 < \beta$, and let $g: \mathbb{R}^2 \rightarrow \mathbb{R}$ be the function defined in $[0, 1]^2$ by

$$(2) \quad g(x, y) = \begin{cases} \alpha, & \text{in } \left] 0, \frac{1}{2} \right[\cup \left] \frac{1}{2}, 1 \right[, \\ \beta, & \text{in } \left(\left] \frac{1}{2}, 1 \right[\times \left] 0, \frac{1}{2} \right[\right) \cup \left(\left] 0, \frac{1}{2} \right[\times \left] \frac{1}{2}, 1 \right[\right), \end{cases}$$

and extended by periodicity in \mathbb{R}^2 . For $\varepsilon > 0$, let $g_\varepsilon(x, y) = g\left(\frac{x}{\varepsilon}, \frac{y}{\varepsilon}\right)$.

We will denote by \mathcal{A}_ε (resp. \mathcal{B}_ε) the union of all closed squares Q of side length ε such that $g_\varepsilon = \alpha$ (resp. $g_\varepsilon = \beta$) in the interior of Q . The set of discontinuity points of g_ε will be denoted by Ξ . A *discontinuity line* is a straight line contained in Ξ .

We define the multifunction G_ε in \mathbb{R}^2 , by setting $G_\varepsilon = [\alpha, \beta]$ on Ξ , and $G_\varepsilon(x, y) = \{g_\varepsilon(x, y)\}$ in $\mathbb{R}^2 \setminus \Xi$.

We want to introduce our notion of geometric evolution $E(t)$, obeying to the law

$$(3) \quad V = \kappa + g_\varepsilon, \quad \text{on } \partial E,$$

where V is the normal velocity, and κ is the crystalline curvature on $\partial E(t)$.

In order to make a sense to (3) it would be enough to require that the evolution is a family of φ -regular sets. Nevertheless, as underlined in Remark 2.2, even if E is a φ -regular set, the crystalline curvature on ∂E may not be uniquely determined, due to the infinitely many choices for the Cahn–Hoffmann vector field on the edges of ∂E .

This ambiguity can be overcome introducing an additional postulate, which is consistent with the notion of forced curve shortening flow (see [3], [4], [5], [22], [23]).

Definition 2.3 (Variational Cahn–Hoffmann field). *A variational Cahn–Hoffmann vector field for a φ -regular set E is a Cahn–Hoffmann vector field n on ∂E such that for every edge L of ∂E not lying on a discontinuity line of g_ε , the restriction n_L of n on L is the unique minimum of the functional*

$$\mathcal{N}_L(n) = \int_L |g_\varepsilon - \operatorname{div} n|^2 d\mathcal{H}^1$$

in the set

$$D_L = \left\{ n \in L^\infty(L, \mathbb{R}^2), n \in T_L, \operatorname{div} n \in L^\infty(L), n(p) = n_0, n(q) = n_1 \right\}$$

where p, q are the endpoints of L and n_0, n_1 are the values at p, q assigned to every Cahn–Hoffmann vector field (see Remark 2.2).

Remark 2.4. If the minimum n_L in D_L of the functional \mathcal{N}_L satisfies the strict constraint $n_L(\xi) \in \operatorname{int} T_L$ for every $\xi \in L$, then the velocity $g_\varepsilon - \operatorname{div} n_L$ is constant along the edge, that is the flat arc remains flat under the evolution. This is always the case for unforced crystalline flows, since the unique minimum is the interpolation of the assigned values at the vertices of L , and the constant value of the φ -curvature is given by

$$\kappa^L = \chi_L \frac{2}{\ell} \text{ on } L,$$

where ℓ is the length of the edge L and χ_L is a convexity factor: $\chi_L = 1, -1, 0$, depending on whether $E(t)$ is locally convex at L , locally concave at L , or neither.

Definition 2.5 (Forced crystalline evolution). Given $T > 0$, we say that a family $E(t)$, $t \in [0, T]$, is a *forced crystalline curvature flow* (or *forced crystalline evolution*) in $[0, T]$ if

- (i) $E(t) \subseteq \mathbb{R}^2$ is a Lipschitz set for every $t \in [0, T]$;
- (ii) there exists an open set $A \subseteq \mathbb{R}^2 \times [0, T]$ such that $\bigcup_{t \in [0, T]} \partial E(t) \times \{t\} \subseteq A$, and the function $d(\xi, t) \doteq d^{E(t)}(\xi)$ is locally Lipschitz in A ;
- (iii) there exists a function $n \in L^\infty(A, \mathbb{R}^2)$, with $\operatorname{div} n \in L^\infty(A)$, such that the restriction of $n(t, \cdot)$ to $\partial E(t)$ is a variational Cahn–Hoffmann vector field for $\partial E(t)$ for almost every $t \in [0, T]$;
- (iv) $\partial_t d - \operatorname{div} n \in G_\varepsilon$ \mathcal{H}^1 -almost everywhere in $\partial E(t)$ and for almost every $t \in [0, T]$.

3. CALIBRABILITY CONDITIONS

In this section we deal with the minimum problem in Definition 2.3 for a given φ -regular set E , and we characterize the edges of ∂E having constant velocity $v_L := \kappa^L + g_\varepsilon$.

The results concern edges $L \in \partial E$ not lying on a discontinuity line of the forcing term, in such a way that g_ε is defined \mathcal{H}^1 -almost everywhere on L . We will use the notation $L = [p, q] \times \{y\}$ or $L = \{x\} \times [p, q]$, with $x, y \notin \frac{\varepsilon}{2}\mathbb{Z}$, so that $\ell = q - p$.

Setting by $n: \mathbb{R} \rightarrow [-1, 1]$ the unique varying component of the variational Cahn–Hoffmann vector field on L (recall Remark 2.2), the assigned values of n are the following:

$$(4) \quad (BV) = \begin{cases} n(p) = n(q) = n_0 \in \{\pm 1\} & \text{if } \chi_L = 0; \\ n(p) = -1, \quad n(q) = 1, & \text{if } \chi_L = 1; \\ n(p) = 1, \quad n(q) = -1, & \text{if } \chi_L = -1. \end{cases}$$

Moreover, we denote by $\gamma_\varepsilon: \mathbb{R} \rightarrow \mathbb{R}$ the restriction of g_ε on the straight line containing L , and we distinguish two different type of discontinuity points for γ_ε :

$$\mathcal{I}_{\beta, \alpha} = \{s \in \mathbb{R}: \gamma_\varepsilon = \alpha \text{ in } (s, s + \varepsilon/2)\}, \quad \mathcal{I}_{\alpha, \beta} = \{s \in \mathbb{R}: \gamma_\varepsilon = \beta \text{ in } (s, s + \varepsilon/2)\}.$$

With these notation, the requirement that $\kappa + g_\varepsilon$ is constant on L can be rephrased in the following 1D problem.

Definition 3.1 (Calibrability conditions). L is a *calibrable edge* of ∂E if and only if there exists a Lipschitz function $n: [p, q] \rightarrow \mathbb{R}$ such that the following hold.

- (i) n satisfies (4).
- (ii) $|n| \leq 1$ in $[p, q]$.
- (iii) $n' + \gamma_\varepsilon = \chi_L \frac{2}{\ell} + \frac{1}{\ell} \int_p^q \gamma_\varepsilon(s) ds$ a.e. in $[p, q]$.

In this case, we say that $v_L = n' + \gamma_\varepsilon$ is the (normal) velocity of the edge L .

The calibrability property was studied, in its full generality, in [10]. We collect here the results needed in the rest of the paper, sketching the proofs for sake of completeness.

Denoting by $\ell_\alpha, \ell_\beta \in [0, \varepsilon/2]$ the non-negative lengths given by the conditions

$$(5) \quad \ell - \varepsilon \left\lfloor \frac{\ell}{\varepsilon} \right\rfloor = \ell_\alpha + \ell_\beta, \quad \int_L \gamma_\varepsilon(s) ds = \frac{\alpha + \beta}{2} (\ell - \ell_\alpha - \ell_\beta) + \alpha \ell_\alpha + \beta \ell_\beta,$$

the calibrability condition in Definition 3.1(iii) sets the value of n' outside the jump set of γ_ε :

$$(6) \quad n'(s) = \begin{cases} \frac{1}{2\ell} (4\chi_L + (\beta - \alpha)(\ell - \ell_\alpha + \ell_\beta)) & \text{if } \gamma_\varepsilon(s) = \alpha, \\ \frac{1}{2\ell} (4\chi_L - (\beta - \alpha)(\ell + \ell_\alpha - \ell_\beta)), & \text{if } \gamma_\varepsilon(s) = \beta. \end{cases}$$

so that n needs to be

$$(7) \quad n(s) = n(p) + (s - p)v_L - \int_p^s \gamma_\varepsilon(\tau) d\tau,$$

where v_L is the feasible velocity of the edge L

$$(8) \quad v_L = \chi_L \frac{2}{\ell} + \frac{\alpha + \beta}{2} + \frac{\beta - \alpha}{2\ell} (\ell_\beta - \ell_\alpha).$$

In conclusion, the calibrability conditions (i) and (iii) in Definition 3.1 fix univocally a candidate field (7) which is continuous and affine with given slope in each phase of γ_ε . This field n is the Cahn–Hoffman field which calibrates L with velocity (8) if and only if it also satisfies the constraint $|n(x)| \leq 1$ for every $x \in [p, q]$.

Remark 3.2. In what follows we will assume $0 < \varepsilon < \frac{8}{\beta - \alpha}$ in such a way that the small perturbation $\chi_L \frac{2}{\ell} + \frac{\beta - \alpha}{2\ell}(\ell_\beta - \ell_\alpha)$ has the same sign of the curvature term $\chi_L \frac{2}{\ell}$.

Proposition 3.3. *Let L be an edge with zero φ -curvature, and let $n_0 \in \{\pm 1\}$ be the given value of the Cahn–Hoffmann vector field at the endpoints of L . Then the following hold.*

- (i) *If $\ell = \ell_\alpha + \ell_\beta < \varepsilon$, L is calibrable with velocity $v_L = \frac{\alpha\ell_\alpha + \beta\ell_\beta}{\ell_\alpha + \ell_\beta}$ if and only if*
 - (ia) $n_0 = 1$, and either $\gamma_\varepsilon(p) = \beta$, $\gamma_\varepsilon(q) = \alpha$, or with an endpoint on $\mathcal{I}_{\alpha,\beta}$;
 - (ib) $n_0 = -1$, and either $\gamma_\varepsilon(p) = \alpha$, $\gamma_\varepsilon(q) = \beta$, or with an endpoint on $\mathcal{I}_{\beta,\alpha}$.
- (ii) *If $\ell \geq \varepsilon$, L is calibrable with velocity $v_L = \frac{\alpha + \beta}{2}$ if and only if*
 - (iia) $n_0 = 1$, and $p, q \in \mathcal{I}_{\alpha,\beta}$;
 - (iib) $n_0 = -1$, and $p, q \in \mathcal{I}_{\beta,\alpha}$.

Proof. If $n_0 = 1$ the Cahn–Hoffmann vector field n needs to be neither increasing near p nor decreasing near q . This occurs only if L is the union of three consecutive segments $L = L_\beta \cup L_c \cup L_\alpha$, with endpoints in p , $p + \ell_\beta \in \mathcal{I}_{\beta,\alpha}$, $q - \ell_\alpha \in \mathcal{I}_{\beta,\alpha}$, and q . If $L_c = \emptyset$, then the candidate field (7) always satisfied the constraint in Definition 3.1(ii), proving (i).

If $L_c \neq \emptyset$, from (7) we get

$$n(p + \varepsilon) - n(p) = \frac{\varepsilon}{2\ell}(\beta - \alpha)(\ell_\beta - \ell_\alpha) = n(q) - n(q - \varepsilon),$$

and hence, since $n(p) = n(q) = 1$, the constraint $|n| \leq 1$ is not satisfied if $\ell_\alpha \neq \ell_\beta$. Finally, if $\ell_\alpha = \ell_\beta$, then, by (6)

$$n'(x) = \begin{cases} \frac{\beta - \alpha}{2} & \text{if } \gamma_\varepsilon(x) = \alpha, \\ \frac{\alpha - \beta}{2} & \text{if } \gamma_\varepsilon(x) = \beta, \end{cases}$$

and a Cahn–Hoffmann vector field with this derivative exists only if $\ell_\alpha = \ell_\beta = \varepsilon/2$, otherwise $n(p + \ell_\beta + \varepsilon/2) > 1$. In conclusion, L is calibrable with velocity $v_L = (\alpha + \beta)/2$ if and only if $p, q \in \mathcal{I}_{\alpha,\beta}$.

The case $n_0 = -1$ follows from similar arguments. \square

Proposition 3.4. *Let L be an edge with positive φ -curvature. If either*

$$(9) \quad \ell + \ell_\alpha - \ell_\beta \leq \frac{4}{\beta - \alpha}$$

or $p \in \mathcal{I}_{\beta,\alpha}$, $q \in \mathcal{I}_{\alpha,\beta}$, then L is calibrable with velocity v_L given by (8).

Proof. Under the assumption (9), the candidate Cahn–Hoffmann vector field (7) is an increasing function in $[p, q]$. Hence the constraint in Definition 3.1(ii) is fulfilled, and L is calibrable.

Assume now that $p \in \mathcal{I}_{\beta,\alpha}$, and $q \in \mathcal{I}_{\alpha,\beta}$. Then the edge has $n(p) = -1$, $n(q) = 1$, $\ell_\alpha = \varepsilon/2$, and $\ell_\beta = 0$. Then, by (6), the candidate Cahn–Hoffmann field (7) is increasing

in $[p, p + \varepsilon/2]$, and, by Remark 3.2,

$$n(p + \varepsilon) - n(p) = \frac{\varepsilon}{4\ell} (8 - (\beta - \alpha)\varepsilon) > 0.$$

Similarly, we obtain that n satisfies the constraint in $[q - \varepsilon, q]$, and hence $|n| \leq 1$ on L , so that L is calibrable with velocity v_L . \square

Remark 3.5. Notice that, if L satisfies the condition (9), then

$$v_L \geq \frac{2}{\ell} + \frac{\alpha + \beta}{2} + \frac{\beta - \alpha}{2\ell} \left(\ell - \frac{4}{\beta - \alpha} \right) = \beta > 0$$

Proposition 3.6. *Let L be an edge with positive φ -curvature, and such that $\ell + \ell_\alpha - \ell_\beta > 4/(\beta - \alpha)$. Then the following hold.*

- (i) *If either $\gamma_\varepsilon(p) = \beta$, or $\gamma_\varepsilon(q) = \beta$, or $p \in \mathcal{I}_{\alpha,\beta}$, or $q \in \mathcal{I}_{\beta,\alpha}$, then L is not calibrable.*
- (ii) *If $\gamma_\varepsilon(p) = \gamma_\varepsilon(q) = \alpha$, let $\sigma_1, \sigma_2 \in (0, \varepsilon/2)$ be such that $p + \varepsilon/2 + \sigma_1 \in \mathcal{I}_{\beta,\alpha}$ and $q - \varepsilon/2 - \sigma_2 \in \mathcal{I}_{\alpha,\beta}$, and let $\tilde{\ell}$ be the length of the interval $[p + \varepsilon/2 + \sigma_1, q - \varepsilon/2 - \sigma_2]$. Setting*

$$m = \varepsilon \frac{\beta - \alpha}{(\beta - \alpha)(\tilde{\ell} + \varepsilon/2) + 4}, \quad h = \frac{\varepsilon(\beta - \alpha)(\tilde{\ell} + \varepsilon/2) - 4}{2(\beta - \alpha)(\tilde{\ell} + \varepsilon/2) + 4},$$

and

$$\Sigma = \left\{ m\sigma_2 + h \leq \sigma_1 \leq \frac{1}{m}\sigma_2 - \frac{h}{m} \right\},$$

we have $m \in (0, 1)$, $\Sigma \cap [0, \varepsilon/2]^2 \neq \emptyset$, and L is calibrable with velocity

$$v_L = \frac{2}{\ell} + \frac{\alpha + \beta}{2} + \frac{\beta - \alpha}{2\ell} \left(\frac{\varepsilon}{2} - \sigma_1 - \sigma_2 \right)$$

if and only if $(\sigma_1, \sigma_2) \in \Sigma$.

- (iii) *if $\gamma_\varepsilon(p) = \alpha$, and $q \in \mathcal{I}_{\alpha,\beta}$ (resp. $p \in \mathcal{I}_{\beta,\alpha}$, and $\gamma_\varepsilon(q) = \alpha$), let $\sigma \in (0, \varepsilon/2)$ be such that $p + \sigma + \varepsilon/2 \in \mathcal{I}_{\beta,\alpha}$ (resp. $q - \sigma - \varepsilon/2 \in \mathcal{I}_{\alpha,\beta}$), let ℓ^* be the length of the interval $[p + \varepsilon/2 + \sigma, q]$ (resp. of $[p, q - \varepsilon/2 - \sigma]$), and let*

$$\sigma^* = \frac{\varepsilon(\beta - \alpha)(\ell^* + \varepsilon/2) - 4}{2(\beta - \alpha)(\ell^* - \varepsilon/2) + 4}.$$

Then L is calibrable if and only if $\sigma \geq \sigma^*$.

Proof. If $\ell + \ell_\alpha - \ell_\beta > 4/(\beta - \alpha)$, by (6) the candidate Cahn–Hoffmann field n is strictly decreasing in the β phase. Hence, under the assumptions in (i), n does not satisfy the constraint $|n| \leq 1$ at least near an endpoint, and L is not calibrable.

If both the endpoints belong to the α phase, then the requirement $(\sigma_1, \sigma_2) \in \Sigma$ is equivalent to the conditions

$$\begin{cases} n(p + \varepsilon/2 + \sigma_1) - n(p) \geq 0, \\ n(q - \varepsilon/2 - \sigma_2) - n(q) \geq 0 \end{cases}$$

that guarantee the calibrability of the edge.

Setting

$$(10) \quad \tilde{\sigma} := \frac{\varepsilon(\beta - \alpha)(\tilde{\ell} + \varepsilon/2) - 4}{2(\beta - \alpha)(\tilde{\ell} - \varepsilon/2) + 4},$$

we have that $(\tilde{\sigma}, \tilde{\sigma}) \in \Sigma$, and $\tilde{\sigma} \in (0, \varepsilon/2)$ under the assumption $\ell + \ell_\alpha - \ell_\beta > 4/(\beta - \alpha)$.

The proof of (iii) follows the same arguments. \square

Remark 3.7 (Calibrability threshold). In the special case when $\sigma_1 = \sigma_2 = \sigma > 0$, the calibrability condition stated in Proposition 3.6(ii) reduces to the unilateral constraint $\sigma \geq \tilde{\sigma}$, where $\tilde{\sigma}$ is the value defined in (10). Hence L is calibrable if and only if $\sigma \geq \tilde{\sigma}$. Moreover, if $\sigma = \tilde{\sigma}$, the edge L is calibrated by a Cahn–Hoffmann vector field n such that $n(p) = n(p + \varepsilon/2 + \tilde{\sigma})$ and $n(q) = n(q - \varepsilon/2 - \tilde{\sigma})$. As a consequence, the same field calibrates both the edges $[p, p + \varepsilon/2 + \tilde{\sigma}] \times \{\bar{y}\}$ and $[q - \varepsilon/2 - \tilde{\sigma}, q] \times \{\bar{y}\}$ (as edges with zero φ -curvature, see Proposition 3.3), and the edge $[p + \varepsilon/2 + \tilde{\sigma}, q - \varepsilon/2 - \tilde{\sigma}] \times \{\bar{y}\}$ (as edges with positive φ -curvature, see Proposition 3.4) with the same velocity.

Similarly, in the case (iii) Proposition 3.6, when $\sigma = \sigma^*$, the edge L is calibrated by a Cahn–Hoffmann vector field n such that $n(p) = n(p + \varepsilon/2 + \sigma^*)$, and the same field calibrates both the edge $[p, p + \varepsilon/2 + \sigma^*] \times \{\bar{y}\}$ (as edge with zero φ -curvature), and the edge $[p + \varepsilon/2 + \tilde{\sigma}, q] \times \{\bar{y}\}$ (as edges with positive φ -curvature) with the same velocity.

4. FORCED CRYSTALLINE FLOWS AND THEIR EFFECTIVE MOTION

The results of Section 3 prescribe a velocity to every calibrable edge not lying on a discontinuity line of g_ε , and suggest that the forced crystalline curvature flow starting from a coordinate polyrectangle (that is a set whose boundary is a closed polygonal curve with edges parallel to the coordinate axes) remains a coordinate polyrectangle, whose structure changes when either existing edges disappear by the growth of their neighbors, or new edges are generated by the splitting of no longer calibrable edges.

In every time interval between these events, the motion is determined by a system of ODEs, and hence the behavior of the evolution on the discontinuities can be described using the general theory of differential equations with discontinuous right-hand side [19].

Concerning the changes of geometry, it is clear what is meant by “disappearing edges”, that is edges whose length becomes zero in finite time, but the notion of “appearing edges”, that is how a no longer calibrable edge breaks, has to be specified.

We focus our attention to coordinate polyrectangles whose edges have non-negative φ -curvature. In the sequel we will use the abuse of notation $L = [p, q]$ when the edge L is of the form $L = [p, q] \times \{y\}$ or $L = \{y\} \times [p, q]$, and $n(p)$, $n(q)$ will denote the prescribed values of the Cahn–Hoffman vector field at the endpoints of L .

Definition 4.1 (Cracking multiplicity and set-up). If L is an edge not lying on a discontinuity line of g_ε , let us define

$$L^c := \sup\{\tilde{L} \subseteq L: \tilde{L} = [s_1, s_2], n(s_1) = n(p), n(s_2) = n(q), \tilde{L} \text{ calibrable}\} = [p_b, q_b],$$

and let us denote by $L^- = [p, p_b]$, $L^+ = [q_b, q]$, with the convention $L^- = \emptyset$ (resp. $L^+ = \emptyset$) if $p = p_b$ (resp. $q = q_b$). The *cracking multiplicity* $M(L)$ assigned to L is given

by

$$M(L) := \begin{cases} 1, & \text{if } L = L^c, \\ 3, & \text{if } L \neq L^c, \text{ and either } L^- = \emptyset, \text{ or } L^+ = \emptyset, \\ 5, & \text{if } L^- \neq \emptyset, \text{ and } L^+ \neq \emptyset. \end{cases}$$

The points p_b, q_b , if different from the endpoints of L , are said *breaking points* of L , and $\mathcal{C}(L) := \{p, p_b, q_b, q\}$ is the *cracking set-up* of L .

For every edge L lying on a discontinuity line of g_ε , with (inner) normal $\nu(L)$, consider the values

$$(11) \quad v_L^{in} = \chi_L \frac{2}{\ell} + \frac{1}{\ell} \int_{L+\frac{\varepsilon}{4}\nu(L)} g_\varepsilon, \quad v_L^{out} = \chi_L \frac{2}{\ell} + \frac{1}{\ell} \int_{L-\frac{\varepsilon}{4}\nu(L)} g_\varepsilon.$$

If $v_L^{in} > 0$ and $v_L^{out} < 0$, then we set $M(L) \in \{1, M(L+\frac{\varepsilon}{4}\nu(L)), M(L-\frac{\varepsilon}{4}\nu(L))\}$. Otherwise, the cracking multiplicity $M(L)$ assigned to L is given by

$$M(L) = \begin{cases} M(L + \frac{\varepsilon}{4}\nu(L)) & \text{if } v_L^{in} > 0 \text{ and } v_L^{out} \geq 0 \\ M(L - \frac{\varepsilon}{4}\nu(L)) & \text{if } v_L^{in} \leq 0 \text{ and } v_L^{out} < 0 \\ 1 & \text{if } v_L^{in} \leq 0 \text{ and } v_L^{out} \geq 0 \end{cases}$$

When $M(L) = M(L \pm \frac{\varepsilon}{4}\nu(L))$, the cracking set-up of L is set as $\mathcal{C}(L) := \mathcal{C}(L \pm \frac{\varepsilon}{4}\nu(L))$.

Proposition 4.2. *Let $L = [p, q]$ be an edge not lying on a discontinuity line of g_ε , and let $\mathcal{C}(L) := \{p, p_b, q_b, q\}$ the cracking set-up of L . Then L^- and L^+ are either empty, or calibrable as edges with zero φ -curvature and prescribed Cahn–Hoffman vector field $n(p) = n(p_b)$, and $n(q_b) = n(q)$, respectively. Moreover, denoting by v^\pm, v^c the velocities of L^\pm, L^c respectively, then*

- (i) $p_b \in \mathcal{I}_{\beta, \alpha}$, $q_b \in \mathcal{I}_{\alpha, \beta}$, and $v^\pm > v^c$, if L has positive φ -curvature;
- (ii) $p_b, q_b \in \mathcal{I}_{\beta, \alpha}$, and $v^- > v^c > v^+$, if L has zero φ -curvature, and $n(p) = -1$;
- (iii) $p_b, q_b \in \mathcal{I}_{\alpha, \beta}$, and $v^- < v^c < v^+$, if L has zero φ -curvature, and $n(p) = 1$;

Proof. Let $L = [p, q]$ be an edge with positive φ -curvature. By Propositions 3.4 and 3.6, if $L^c \neq L$ then $\ell + \ell_\alpha - \ell_\beta > 4/(\beta - \alpha)$, and

$$p_b = \min\{s \in [p, q] \cap \mathcal{I}_{\beta, \alpha}\}, \quad q_b = \max\{s \in [p, q] \cap \mathcal{I}_{\alpha, \beta}\},$$

Moreover, by Proposition 3.3, $L^- = [p, p_b] \subseteq L$ is either empty or calibrable as edge with zero φ -curvature and prescribed Cahn–Hoffmann $n_0 = -1$ at the endpoints. Similarly $L^+ = [q_b, q] \subseteq L$ is either empty or calibrable as edge with zero φ -curvature and prescribed Cahn–Hoffmann $n_0 = -1$ at the endpoints.

Concerning the velocities, assume that $p \neq p_b$. If either $\gamma_\varepsilon(p) = \beta$ or $p \in \mathcal{I}_{\alpha, \beta}$, we have $v^- = \beta > v^c$, by Remark 3.5. If $\gamma_\varepsilon(p) = \alpha$, then, by Proposition 3.3(i),

$$v^- = v(\sigma) = \frac{\sigma\alpha + \frac{\varepsilon}{2}\beta}{\sigma + \frac{\varepsilon}{2}}$$

with $0 < \sigma < \sigma_0$, where σ_0 is such that $v(\sigma_0) = v^c$ (see also Remark 3.7). The inequality $v^- > v^c$ then follows from the fact that the function $v(\sigma)$ is strictly monotone decreasing. The same arguments can be used for v^+ in the case $q_b \neq q$.

Recalling Proposition 3.3, we can perform a similar splitting for edges with zero φ -curvature. If $q - p \geq \varepsilon$, then, if $n(p) = n(q) = 1$, we have

$$p_b = \min\{s \in [p, q] \cap \mathcal{I}_{\alpha, \beta}\}, \quad q_b = \max\{s \in [p, q] \cap \mathcal{I}_{\alpha, \beta}\},$$

while, if $n(p) = n(q) = -1$, we have

$$p_b = \min\{s \in [p, q] \cap \mathcal{I}_{\beta, \alpha}\}, \quad q_b = \max\{s \in [p, q] \cap \mathcal{I}_{\beta, \alpha}\}.$$

In both cases the remaining parts L^\pm are either empty or calibrable with velocities

$$v^\pm = \frac{\sigma_\alpha^\pm \alpha + \sigma_\beta^\pm \beta}{\sigma_\alpha^\pm + \sigma_\beta^\pm},$$

for suitable $\sigma_\alpha^\pm, \sigma_\beta^\pm \in [0, \varepsilon/2]$. Since $v^c = \frac{\alpha + \beta}{2}$, the strict inequalities in (ii) and (iii) hold true.

The case of L with zero φ -curvature and $q - p < \varepsilon$ is similar and is left to the reader. We would like to stress that the edges of this type appearing as L^\pm , due to the cracking set-up, are always calibrable. \square

Definition 4.3 (Breaking configuration). Let E be a coordinate polyrectangle whose edges $\tilde{L}_1, \dots, \tilde{L}_n$ have non-negative φ -curvature. For every $i = 1, \dots, n$, let $\mathcal{C}(L_i) = \{p_i, p_{i,b}, q_{i,b}, q_i\}$ be a cracking set-up of the edge \tilde{L}_i . The *breaking configuration* of ∂E associated to $\{\mathcal{C}(\tilde{L}_i)\}_{i=1}^n$ is given by L_1, \dots, L_m , $m = \sum_{i=1}^n M(\tilde{L}_i)$, where L_j is either a part of an edge \tilde{L}_i obtained by the splitting procedure in Definition 4.1, or a degenerate segment with length zero at a cracking point $p_{i,b}$ or $q_{i,b}$.

Remark 4.4. By Proposition 4.2, a breaking configuration of the boundary of a coordinate polyrectangle E , whose edges have non-negative φ -curvature always exists. Moreover, since the cracking multiplicity and set-up of an edge L is unambiguous except in the case $v_L^{in} > 0$ and $v_L^{out} < 0$, the breaking configuration is unique, provided that no edge $L \subseteq \partial E$ has $v_L^{in} > 0$ and $v_L^{out} < 0$.

The following result shows that, in our setting, the evolution is well posed.

Proposition 4.5. *Let E be a coordinate polyrectangle whose edges have non-negative φ -curvature, and let L_1, \dots, L_m a breaking configuration of ∂E . Then there exists $T > 0$ and a family $E(t)$, $t \in [0, T]$ of coordinate polyrectangles with edges $L_1(t), \dots, L_m(t)$ which is a forced crystalline flow starting from E . If, in addition, every L_i with positive length and lying on a discontinuity line of g_ε satisfies one of the following properties*

- (1) $v_{L_i}^{in} < 0$, and $v_{L_i}^{out} > 0$,
- (2) $v_{L_i}^{in} > 0$ and $v_{L_i}^{out} > 0$,
- (3) $v_{L_i}^{in} < 0$ and $v_{L_i}^{out} < 0$,

then the evolution is unique. Moreover if L_i satisfies condition (1), then $L_i(t)$ is pinned until $v_{L_i(t)}^{in} \leq 0$ and $v_{L_i(t)}^{out} \geq 0$.

Proof. A given coordinate polyrectangle E , with edges $\tilde{L}_1, \dots, \tilde{L}_n$, is completely determined by the strings $(\tilde{\nu}_1, \dots, \tilde{\nu}_n)$ and $(\tilde{s}_1, \dots, \tilde{s}_n)$, where $\tilde{\nu}_i$ and \tilde{s}_i are the inner normal vector and the distance from the origin of the edge L_i , $i = 1, \dots, n$, respectively.

Let us denote $e_1 = e_5 = (1, 0)$, $e_2 = (0, 1)$, $e_3 = (-1, 0)$, and $e_4 = e_0 = (0, -1)$, so that if $\tilde{\nu}_i = e_j$, then $\tilde{\nu}_{i+1} \in \{e_{j-1}, e_{j+1}\}$.

We associate to E a breaking configuration (ν_1, \dots, ν_m) , (s_1, \dots, s_m) based on the cracking set-up of its edges in the following way.

If $M(L_1) = 1$, then $\nu_1 = \tilde{\nu}_1$ and $s_1 = \tilde{s}_1$. If $M(L_1) = 3$, $q_{1,b} = q_1$, and $\nu_1 = e_j$ then $(\nu_1, \nu_2, \nu_3) = (e_j, e_{j+1}, e_j)$ and $(s_1, s_2, s_3) = (\tilde{s}_1, p_{1,b}, \tilde{s}_1)$. Similarly, if $M(L_1) = 3$, $p_{1,b} = p_1$, and $\nu_1 = e_j$ then $(\nu_1, \nu_2, \nu_3) = (e_j, e_{j-1}, e_j)$ and $(s_1, s_2, s_3) = (\tilde{s}_1, q_{b,1}, \tilde{s}_1)$. Finally, if $M(L_1) = 5$, then $(\nu_1, \nu_2, \nu_3, \nu_4, \nu_5) = (e_j, e_{j+1}, e_j, e_{j-1}, e_j)$ and $(s_1, s_2, s_3, s_4, s_5) = (\tilde{s}_1, p_{1,b}, \tilde{s}_1, q_{1,p}, \tilde{s}_1)$. The subsequent elements of the strings are obtained applying the same procedure to L_2 , and so forth.

By Definition 2.5, a forced crystalline flow $E(t)$, $t \in [0, T]$ given by calibrable coordinate polyrectangles with edges $L_1(t), \dots, L_m(t)$ and with normal direction (ν_1, \dots, ν_m) , is then identified with a solution $s(t) = (s_1(t), \dots, s_m(t))$ to the system of ODEs

$$(12) \quad s' = V(s) \quad \text{in } [0, T]$$

where $V: \mathbb{R}^m \rightarrow \mathbb{R}^m$ is the field, discontinuous on

$$\Sigma = \left\{ s \in \mathbb{R}^m : \exists s_i \in \frac{\varepsilon}{2}\mathbb{Z} \right\},$$

and defined outside Σ by

$$V = (V_1, \dots, V_m), \quad V_i(s) = - \left(\chi_{L_i} \frac{2}{\ell_i(s)} + \frac{1}{\ell_i(s)} \int_{L_i(s)} g_\varepsilon \right), \quad i = 1, \dots, m, \quad s \notin \Sigma.$$

Notice that the fictitious edges with zero length, possibly added in the breaking configuration of E , are contained on discontinuity lines of g_ε . Then either E is calibrable, or it corresponds to a string $s \in \Sigma$.

System (12) fits therefore into Filippov's theory of discontinuous dynamical systems (see [19], [13]): the field V is extended on Σ by the multifunction

$$(13) \quad F(V)(s) = \text{co} \left\{ \lim_{k \rightarrow \infty} V(s^k), s^k \rightarrow s, s^k \notin \Sigma \right\}, \quad s \in \Sigma,$$

(where we denote by $\text{co}(A)$ the convex envelope of a set A) and a solution of (12) is, by definition, a solution of the differential inclusion $s' \in F(V)(s)$. Since $V: \mathbb{R}^m \rightarrow \mathbb{R}^m$ is measurable and essentially bounded, then there exists at least a solution of such a differential inclusion, starting from any initial datum s .

In order to deal with the uniqueness of solutions, we need an explicit computation of the multifunction $F(V)$ on Σ .

For every $s \in \Sigma$, and for every component s_i of s such that $s_i \in \frac{\varepsilon}{2}\mathbb{Z}$, and $s_{i-1} \neq s_{i+1}$, so that $\ell_i(s) > 0$, let $V_i^+(s)$ and $V_i^-(s)$ be the values

$$V_i^+(s) = - \left(\chi_{L_i} \frac{2}{\ell_i(s)} + \frac{1}{\ell_i(s)} \int_{L_i(s) + \frac{\varepsilon}{4}\nu_i} g_\varepsilon \right),$$

$$V_i^-(s) = - \left(\chi_{L_i} \frac{2}{\ell_i(s)} + \frac{1}{\ell_i(s)} \int_{L_i(s) - \frac{\varepsilon}{4}\nu_i} g_\varepsilon \right),$$

and let $I(V_i^-(s), V_i^+(s))$ be the interval with endpoints $V_i^-(s)$ and $V_i^+(s)$.

For every $i = 1, \dots, m$, $V_i(s)$ depends only on s_{i-1} , s_i , and s_{i+1} , and it is discontinuous only in the s_i variable, then $F(V)(s)$ in (13) is the convex set

$$F(V)(s) = I_1(s) \times \dots \times I_m(s)$$

where

$$I_i(s) = \begin{cases} \{V_i(s)\}, & \text{if } s_i \notin \frac{\varepsilon}{2}\mathbb{Z}, \\ I(V_i^-(s), V_i^+(s)) & \text{if } s_i \in \frac{\varepsilon}{2}\mathbb{Z}, \text{ and } \ell_i > 0 \\ [\alpha, \beta] & \text{if } s_i \in \frac{\varepsilon}{2}\mathbb{Z}, \text{ and } \ell_i = 0, \end{cases} \quad i = 1, \dots, m.$$

Assume now that every element of the breaking configuration of ∂E with positive length satisfies one of the conditions (1), (2), (3).

Concerning the edges with zero length, notice that if $L_i(t)$ is an edge starting from L_i with $\ell_i = 0$, then $\ell_i(t) > 0$ and $v_{L_i(t)}^{in} = \alpha$, $v_{L_i(t)}^{out} = \beta$ for $t > 0$ small enough, so that the edge $L_i(t)$ fulfills (1). Hence we can split the indices $\{1, \dots, m\} = \mathcal{N}_1 \cup \mathcal{N}_2 \cup \mathcal{N}_3$ in such a way $L_i(t)$ satisfies (j) for every $i \in \mathcal{N}_j$, locally near $t = 0$.

Let s^0 be the string corresponding to the breaking configuration of ∂E , let $E(t)$ be any evolution obtained by solving the differential inclusion (12) with initial datum $s(0) = s^0$, and let $\bar{t} \in (0, T]$ be such that $L_i(t)$ satisfies (j) in $(0, \bar{t})$ for every $i \in \mathcal{N}_j$, $j = 1, 2, 3$. The family $E(t)$ is then identified with $s(t) = (s_1(t), \dots, s_m(t))$ solving $s'_i(t) \in I_i(s(t))$ a.e. in $(0, \bar{t})$, $i = 1, \dots, m$.

Then, for every $i \in \mathcal{N}_1$, we have that $s'_i(s_i - s_i(0)) \leq 0$ for every choice of $s'_i(t) \in I_i(s(t)) = I(V_i^-(s(t)), V_i^+(s(t)))$, and hence $s'_i = 0$ in $(0, \bar{t})$. (see, e.g., [19] Corollary 2.10.2).

On the other hand, for every $i \in \mathcal{N}_2 \cup \mathcal{N}_3$, then either $s'_i > 0$ or $s'_i < 0$ in $(0, \bar{t})$, and hence $s_i(t) = \{V_i(s(t))\}$ a.e. in $(0, \bar{t})$.

In conclusion, since the function V is Lipschitz continuous outside Σ , the solution of the differential inclusion is unique in $(0, \bar{t})$, and it is fully determined by the law

$$s'_i = \begin{cases} 0 & i \in \mathcal{N}_1 \\ V_i(s) & i \in \mathcal{N}_2 \cup \mathcal{N}_3. \end{cases} \quad \text{a.e. in } (0, \bar{t}).$$

In terms of the breaking configuration of ∂E , we can conclude that every edge L_i , with $i \in \mathcal{N}_2 \cup \mathcal{N}_3$ crosses immediately the discontinuity line, moving inward (respectively outward) if $i \in \mathcal{N}_2$ (respectively $i \in \mathcal{N}_3$), while every edge L_i with $i \in \mathcal{N}_1$ is pinned on the discontinuity line. \square

Remark 4.6. As a consequence of Proposition 4.5, if $\alpha + \beta < 0$, for every $\varepsilon > 0$ there are nontrivial equilibria of the forced crystalline curvature flow. For example, a calibrable coordinate polyrectangle E such that

- (a) every vertex of E is also a vertex of a square $Q \in \mathcal{A}_\varepsilon$, $Q \subseteq E$,
- (b) every edge of ∂E with zero φ -curvature has length $\ell = \varepsilon/2$,
- (c) every edge of ∂E with positive φ -curvature has length ℓ very closed to $-4/(\alpha + \beta)$,

is pinned. Namely, requirement (a) implies that every edge of ∂E lies on a discontinuity line, (b) guarantees that $v_L^{in} = \alpha$ and $v_L^{out} = \beta$ for every edge L with zero φ -curvature,

while (c) guarantees that

$$v_L^{in} = \frac{2}{\ell} + \frac{\alpha + \beta}{2} - \frac{(\beta - \alpha)\varepsilon}{4\ell} < 0, \quad v_L^{out} = \frac{2}{\ell} + \frac{\alpha + \beta}{2} + \frac{(\beta - \alpha)\varepsilon}{4\ell} > 0.$$

for every edge L with positive φ -curvature.

In particular, the symmetric equilibria O_ε (see Figure 1) converge, as $\varepsilon \rightarrow 0$ to an octagon O having horizontal and vertical edges with length $\ell = -4/(\alpha + \beta)$, connected by diagonal edges.

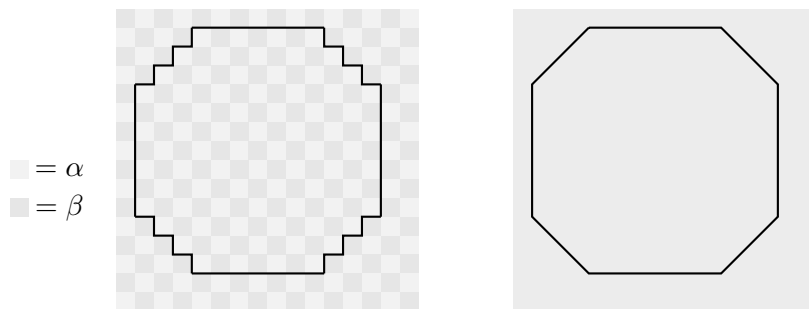


FIGURE 1. Microscopic and macroscopic nontrivial equilibrium ($\alpha + \beta < 0$).

In conclusion, the forced crystalline evolutions defined in Definition 2.5 and starting from a polyrectangle are obtained by the following procedure: we set-up the initial datum and we obtain the evolution $E(t)$ by solving the system of ODEs (12), for $t \in [0, T]$, where $T > 0$ is the first time when an edge either disappears or is no more calibrable. The subsequent evolution is obtained by initializing $E(T)$ according to Definition 4.1 as an initial datum for the new system of ODEs of the form (12).

We are interested in stressing the macroscopic effect of the underlying periodic structure on the geometric evolutions, depicting clearly the forced crystalline flows and passing to the limit as $\varepsilon \rightarrow 0$, and the most of the features are revealed by the evolution starting from the simplest crystals: the coordinate squares.

In what follows $S(\ell)$ will denote a coordinate square with side length $\ell > 0$.

Theorem 4.7 (Effective motion of coordinate squares). *Let $S(\ell_0)$ be a given coordinate square. For every $\varepsilon > 0$, let $S(\ell_0^\varepsilon)$ be a coordinate square such that $d_H(S(\ell_0), S(\ell_0^\varepsilon)) < \varepsilon$. Then there exists a forced crystalline curvature flow $E^\varepsilon(t)$, $t \in [0, T)$, starting from $S(\ell_0^\varepsilon)$. Moreover, there exists a family of sets $E(t)$, $t \in [0, T)$, such that $E^\varepsilon(t)$ converges to $E(t)$ in the Hausdorff topology and locally uniformly in time, as $\varepsilon \rightarrow 0$. The limit evolution $E(t)$ is independent of the choice of the approximating initial data $S(\ell_0^\varepsilon)$, but its geometry depends on ℓ_0 in the following way.*

- (i) *If either $\alpha + \beta \geq 0$ and $\ell_0 > 0$ or $\alpha + \beta < 0$ and $0 < \ell_0 \leq -4/(\alpha + \beta)$, then $E(t)$ is a family of coordinate squares $E(t) = S(\ell(t))$, with $\ell(t)$ governed by the ODE*

$$(14) \quad \begin{cases} \ell' = -\frac{4}{\ell} - (\alpha + \beta), \\ \ell(0) = \ell_0, \end{cases}$$

and then shrinking to a point in finite time.

- (ii) If $\alpha + \beta < 0$ and $\ell_0 > -4/(\alpha + \beta)$, then $E(t)$ is a family of octagons $E(t) = S(\ell_0)^\circ \cap S(\tilde{\ell}(t))$, where $S(\ell_0)^\circ$ is the polar square of $S(\ell_0)$, and $\tilde{\ell}(t)$ is the solution to (14). In particular, the moving edges of $E(t)$ have length governed by the ODE

$$(15) \quad \begin{cases} \ell' = \frac{4}{\ell} + (\alpha + \beta), \\ \ell(0) = \ell_0, \end{cases}$$

and then $E(t)$ is increasing in $[0, +\infty)$, and converging to a stationary octagon as $t \rightarrow +\infty$.

Proof. Given $S(\ell_0)$ and $\varepsilon > 0$, let $S(\ell_0^\varepsilon)$ be a square such that $d_H(S(\ell_0), S(\ell_0^\varepsilon)) < \varepsilon$.

Case (i)a: $\ell_0 \leq 4/(\beta - \alpha)$ (self-similar shrinking).

By Proposition 3.4, the breaking configuration of $\partial S(\ell_0^\varepsilon)$ has no breaking points, and, by Remark 3.5 either $v_L^{in}, v_L^{out} > 0$, if $L \subseteq \partial S(\ell_0^\varepsilon)$ is on a discontinuity line of g_ε , or $v_L > 0$, otherwise. Then, by Remark 4.4, and Proposition 4.5, there exists a unique forced crystalline flow $E^\varepsilon(t)$ starting from $S(\ell_0)$, and it is given by calibrable squares $S(\ell^\varepsilon(t))$ with side length governed by the ODE

$$(16) \quad (\ell^\varepsilon)' = -\frac{4}{\ell^\varepsilon} - (\alpha + \beta) - \frac{\beta - \alpha}{\ell^\varepsilon}(\ell_\beta^\varepsilon - \ell_\alpha^\varepsilon).$$

Since $|\ell_\beta^\varepsilon - \ell_\alpha^\varepsilon| \leq \varepsilon/2$, a passage to the limit in (16) as $\varepsilon \rightarrow 0$ shows that $E^\varepsilon(t)$ converges in the Hausdorff topology and locally uniformly in time to the family of squares $S(\ell(t))$ with side length governed by the ODE (14).

Case (i)b: either $\ell_0 > 4/(\beta - \alpha)$ (if $\alpha + \beta \geq 0$), or $4/(\beta - \alpha) < \ell_0 \leq -4/(\alpha + \beta)$ (if $\alpha + \beta < 0$) (shrinking with temporary breaking).

As a first step, we assume, in addition, that every vertex of $S(\ell_0^\varepsilon)$ is also a vertex of a square $Q \in \mathcal{A}_\varepsilon$, $Q \subseteq S(\ell_0^\varepsilon)$ (see Figure 2(I)), so that the edges lie on discontinuity lines of g_ε and they have (the same) velocities $v_{0,\varepsilon}^{in}, v_{0,\varepsilon}^{out} \geq 0$. Hence, by Definition 4.1 and Proposition 3.4, we have

$$M(L^\varepsilon) = M\left(L^\varepsilon + \frac{\varepsilon}{4}\nu(L^\varepsilon)\right) = 1, \quad \forall L^\varepsilon \subseteq \partial S(\ell_0^\varepsilon),$$

and, by Proposition 4.5, there exists a unique forced crystalline flow starting from $S(\ell_0^\varepsilon)$, given by squares $S(\ell^\varepsilon(t))$ with side length governed by the ODE (16), and defined in $(0, t_0)$ where

$$t_0 = \sup\{t > 0: S(\ell(s)) \text{ is calibrable for every } s \in (0, t)\}$$

(see Figure 2(II)). By symmetry, the breaking set-up of every edge of $E(t_0) = S(\ell(t_0))$ is the same, and it is given by Proposition 4.2(i). More precisely, every edge $L_i^\varepsilon(t_0)$ has cracking multiplicity $M(L_i^\varepsilon(t_0)) = 5$, and set-up $\mathcal{C}(L_i^\varepsilon(t_0)) = \{p_i, p_{i,b}, q_{i,b}, q_i\}$ with

$$\frac{\varepsilon}{2} + \tilde{\sigma} = |p_i - p_{i,b}| = |q_i - q_{i,b}| = |p_j - p_{j,b}| = |q_j - q_{j,b}| \quad \forall i, j = 1, \dots, 4,$$

where $\tilde{\sigma}$ is the calibrability threshold defined in (10). Moreover, by Remark 3.7, using the notation of Proposition 4.2, we have $L_i^\varepsilon(t_0) = L_i^+ \cup L_i^c \cup L_i^-$, and $v^+ = v^- = v^c$.

Then, by Proposition 4.5, the evolution admits a unique extension $E^\varepsilon(t)$, given by polyrectangles with 20 edges, and defined for $t \in (t_0, t_1)$, where t_1 is the first time when an edge of $E^\varepsilon(t)$ touches a discontinuity line of g_ε . By symmetry, the evolution in (t_0, t_1) is fully depicted by its behavior near a vertex of $S(\ell^\varepsilon(t_0))$ (see Figure 2(III)): pinned edges with zero φ -curvature are generated in the normal direction of the edges of $S(\ell^\varepsilon(t_0))$ at the breaking points, while the edges parallel to the edges of $S(\ell^\varepsilon(t_0))$ move inward. More precisely, the edges with positive φ -curvature move inward with constant velocity

$$(17) \quad v_c^\varepsilon = \frac{2}{\ell_0^\varepsilon - 2\varepsilon} + \frac{\alpha + \beta}{2} + \frac{(\alpha - \beta)\varepsilon}{\ell_0^\varepsilon - 2\varepsilon},$$

while the small edges with zero φ -curvature move inward with velocity $v_\pm^\varepsilon(t) > v_c^\varepsilon$, and reach a discontinuity line at time t_1 (see Figure 2(IV)). Every edge $S(\ell^\varepsilon(t_1))$ lying on a discontinuity line of g_ε has zero φ -curvature, and $v^{in} = \alpha$, $v^{out} = \beta$, and, by Proposition 4.5, there exists a unique extension of the evolution after t_1 , given by polyrectangles with pinned edges with zero φ -curvature, and moving edges with positive φ -curvature. If we denote by t_2 the first time when those edges reach the discontinuity lines, in such a way that $E^\varepsilon(t_2)$ becomes again a square $S(\ell_0^\varepsilon - 2\varepsilon)$, then we have

$$\varepsilon > v_c^\varepsilon(t_2 - t_1) > (k + o(\varepsilon))(t_2 - t_1),$$

where k is a constant independent of ε , and hence the evolution recomposes the square in a time lapse of order ε (see Figure 2(V)).

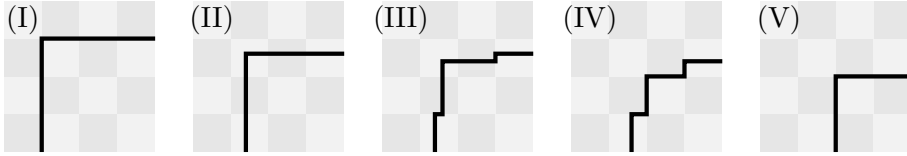


FIGURE 2. The breaking and recomposing phenomenon

Since $E^\varepsilon(t_2)$ is a square with every vertex which is also a vertex of a square $Q \in \mathcal{A}_\varepsilon$, $Q \subseteq S(\ell_0^\varepsilon)$, the (unique) evolution then either iterates this “breaking and recomposing” motion, if $\ell^\varepsilon(t_2) = \ell_0^\varepsilon - 2\varepsilon > 4/(\beta - \alpha)$, or it is a family of shrinking squares, if $\ell^\varepsilon(t_2) \leq 4/(\beta - \alpha)$. In any case, $E^\varepsilon(t)$ can be approximate, in the Hausdorff topology and locally uniformly in time, by a family of squares with side length satisfying (16), so that the limit motion as $\varepsilon \rightarrow 0$ is a family of squares $S(\ell(t))$ governed by the evolution law (14).

Moreover, for every square $S(\ell_0^\varepsilon)$ such that $d_H(S(\ell_0), S(\ell_0^\varepsilon)) < \varepsilon$, the forced crystalline evolution generates and absorbs the small edges near its corners in slightly different ways, but it is always approximable by a family of squares with side length satisfying (16). In particular, the limit evolution does not depend on the choice of the approximating data.

Case (ii): $\alpha + \beta < 0$, and $\ell_0 > -4/(\alpha + \beta)$ (confinement).

If every vertex of $S(\ell_0^\varepsilon)$ is also a vertex of a square $Q \in \mathcal{A}_\varepsilon$, $Q \subseteq S(\ell_0^\varepsilon)$ (see Figure 3(I)), then the edges of the square lie on discontinuity lines of g_ε , and they have the

same velocities $v_{0,\varepsilon}^{in}, v_{0,\varepsilon}^{out} < 0$. Hence, by Definition 4.1 and Proposition 3.4, we have

$$M(L^\varepsilon) = M\left(L^\varepsilon - \frac{\varepsilon}{4}\nu(L^\varepsilon)\right) = 5, \quad \forall L^\varepsilon \subseteq \partial S(\ell_0^\varepsilon),$$

and, by Proposition 4.2, every edge of $S(\ell_0^\varepsilon)$ is splitted as $L_i^\varepsilon = L_i^+ \cup L_i^c \cup L_i^-$ with $v_\pm^{in} = \alpha$, $v_\pm^{out} = \beta$, and $v_c^{in}, v_c^{out} < 0$. Then, by Proposition 4.5, there exists a unique forced crystalline flow starting from $S(\ell_0^\varepsilon)$ (see Figure 3(II)), producing small pinned corners having edges with zero φ -curvature and length $\varepsilon/2$, while the long edges with positive φ -curvature move outward with constant velocity v_c given by (17) until they reach the next discontinuity line (see Figure 3(III)).

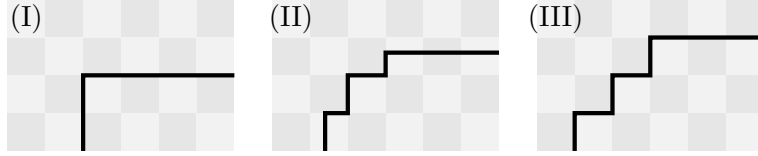


FIGURE 3. The cutting phenomenon

Then the process iterates, “cutting” the square and reducing the length $\ell^\varepsilon(t)$ of the edges with positive φ -curvature, so that their (piecewise constant) velocity is given by

$$v^\varepsilon(t) = \frac{2}{\ell^\varepsilon(t)} + \frac{\alpha + \beta}{2} - \frac{(\beta - \alpha)\varepsilon}{4\ell^\varepsilon(t)},$$

until the first time t_0 when $|v^\varepsilon(t_0) + 4/(\alpha + \beta)| < \varepsilon$. By Proposition 4.5 (see also Remark 4.6) every edge of $E^\varepsilon(t)$ is pinned for $t > t_0$. In conclusion, if we denote by $E(t)$ the family of octagons $E(t) = S(\ell_0)^\circ \cap S(\tilde{\ell}(t))$, where $S(\ell_0)^\circ$ is the polar square of $S(\ell_0)$, and $\tilde{\ell}(t)$ is the solution to (14), we have $d_H(E^\varepsilon(t) - E(t)) \leq c\varepsilon$, so that $E^\varepsilon(t)$ converges to $E(t)$ in the Hausdorff topology and locally uniformly in time, as $\varepsilon \rightarrow 0$.

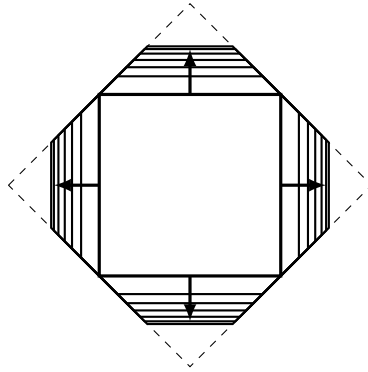


FIGURE 4. The effective evolution in Case 2 of confinement.

Finally, notice that the forced crystalline evolution starting from a general initial datum $S(\ell_0^\varepsilon)$, with $d_H(S(\ell_0), S(\ell_0^\varepsilon)) < \varepsilon$, reaches a configuration of the type depicted

in Figure 3(III) in a time span of order ε . Then the macroscopic limit $E(t)$ does not depend on the choice of the approximating initial datum, and it is the effective motion of the square $S(\ell_0)$. \square

The arguments used in the proof of Theorem 4.7 can be performed to deal with every polyrectangle (and hence, by approximation, to describe the effective evolution of general sets), but a detailed analysis of the forced crystalline flow in these cases requires considerable additional computation. Just to appreciate the application of the previous arguments in a slightly more general setting, we devote the end of this section to a concise description of the motion starting from coordinate rectangles.

In what follows $R(\ell_1, \ell_2)$ will denote a coordinate rectangle with side lengths $\ell_1, \ell_2 > 0$. Having already characterized the evolution of a square, without loss of generality we can assume that $\ell_{1,0} > \ell_{2,0}$.

Theorem 4.8 (Effective motion of coordinate rectangles). *Let $R(\ell_{1,0}, \ell_{2,0})$ be a given coordinate rectangle. For every $\varepsilon > 0$, let $R(\ell_{1,0}^\varepsilon, \ell_{2,0}^\varepsilon)$ be a coordinate rectangle such that $d_H(R(\ell_{1,0}, \ell_{2,0}), R(\ell_{1,0}^\varepsilon, \ell_{2,0}^\varepsilon)) < \varepsilon$. Then there exists a forced crystalline curvature flow $E^\varepsilon(t)$, $t \in [0, T)$, starting from $R(\ell_{1,0}^\varepsilon, \ell_{2,0}^\varepsilon)$. Moreover, there exists a family of sets $E(t)$, $t \in [0, T)$, such that $E^\varepsilon(t)$ converges to $E(t)$ in the Hausdorff topology and locally uniformly in time, as $\varepsilon \rightarrow 0$. The limit evolution $E(t)$ is independent of the choice of the approximating initial data $R(\ell_{1,0}^\varepsilon, \ell_{2,0}^\varepsilon)$, but its geometry depends on the values*

$$v_{i,0} := \frac{2}{\ell_{i,0}^\varepsilon} + \frac{\alpha + \beta}{2}, \quad i = 1, 2$$

in the following way.

- (i) If $v_{i,0} \geq 0$, $i = 1, 2$, then $E(t)$ is a family of rectangles $E(t) = R(\ell_1(t), \ell_2(t))$ with $\ell_i(t)$ governed by the system of ODEs

$$(18) \quad \begin{cases} \ell_1' = -\frac{4}{\ell_2} - (\alpha + \beta), \\ \ell_2' = -\frac{4}{\ell_1} - (\alpha + \beta), \\ \ell_1(0) = \ell_{1,0}, \\ \ell_2(0) = \ell_{2,0}. \end{cases}$$

- (ii) If either $v_{i,0} < 0$, $i = 1, 2$, or $v_{1,0} < 0$, $v_{2,0} \geq 0$ and $v_{1,0} + v_{2,0} \leq 0$, then $E(t)$ is a family of octagons $E(t) = Q(R(\ell_{1,0}, \ell_{2,0})) \cap R(\tilde{\ell}_1(t), \tilde{\ell}_2(t))$, where $Q(R(\ell_{1,0}, \ell_{2,0}))$ is the rotated square touching from outside $R(\ell_{1,0}, \ell_{2,0})$ at its vertices, and $(\tilde{\ell}_1, \tilde{\ell}_2)$ is the solution to (18). In particular, the lengths of the moving edges of $E(t)$ are governed by the system of ODEs

$$(19) \quad \begin{cases} \ell_1' = \frac{4}{\ell_1} + (\alpha + \beta), \\ \ell_2' = \frac{4}{\ell_2} + (\alpha + \beta), \\ \ell_1(0) = \ell_{1,0}, \\ \ell_2(0) = \ell_{2,0}. \end{cases}$$

(iii) If $v_{1,0} < 0$, $v_{2,0} \geq 0$ and $v_{1,0} + v_{2,0} > 0$, then there exists $T > 0$ such that, for $t \in [0, T]$, $E(t)$ is a family of rectangles $E(t) = R(\ell_1(t), \ell_2(t))$ with $\ell_i(t)$ governed by the system of ODEs (18). If $T = +\infty$, then $E(t)$ converges to an equilibrium (either a point or the square $S(-4/(\alpha + \beta))$) for $t \rightarrow +\infty$. If $T < +\infty$, $E(t)$, $t \in [0, T)$, is the family of octagons following the rules of case (ii).

Proof. When either $v_{i,0} \geq 0$, or $v_{i,0} < 0$, $i = 1, 2$, the proof is very similar to the one of Theorem 4.7, hence we address our attention to initial data with $v_{1,0} \leq 0$ and $v_{2,0} > 0$ (mixed case).

Assume that every vertex of the approximating initial datum $R(\ell_{1,0}^\varepsilon, \ell_{2,0}^\varepsilon)$ is also a vertex of a square $Q \in \mathcal{A}_\varepsilon$, $Q \subseteq R(\ell_{1,0}^\varepsilon, \ell_{2,0}^\varepsilon)$. By symmetry, it is enough depict the evolution of two contiguous edges L_1^ε (horizontal) and L_2^ε (vertical) starting as in Figure 5. We have that $v_{L_1^\varepsilon}^{in}, v_{L_1^\varepsilon}^{out} \leq 0$, so that

$$M(L_1^\varepsilon) = M\left(L_1^\varepsilon - \frac{\varepsilon}{4}\nu(L_1^\varepsilon)\right) = 3,$$

while $v_{L_2^\varepsilon}^{in}, v_{L_2^\varepsilon}^{out} \geq 0$, and

$$M(L_2^\varepsilon) = M\left(L_2^\varepsilon + \frac{\varepsilon}{4}\nu(L_2^\varepsilon)\right) = 1.$$

Therefore the forced evolution starts breaking the edge L_1^ε , and generating small pinned edges with zero φ -curvature (see Figure 5(II)). The edges with positive curvature move with constant velocities v_1^ε (outward) and v_2^ε (inward).

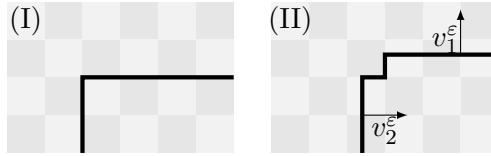


FIGURE 5. How the mixed case starts.

Setting

$$(20) \quad U(\ell_1, \ell_2) := \frac{1}{\ell_1} + \frac{1}{\ell_2} + \frac{\alpha + \beta}{2},$$

the subsequent evolution depends on the sign of $U_0 = U(\ell_{1,0}, \ell_{1,0})$ (note that $\alpha + \beta < 0$ in this case).

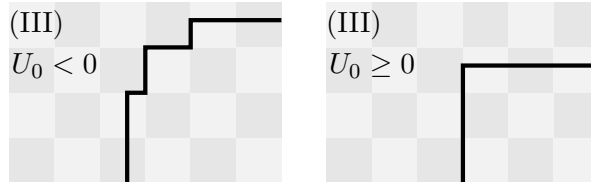


FIGURE 6. How the mixed case carries on.

If $U_0 < 0$, so that $v_2^\varepsilon < -v_1^\varepsilon$, the small pinned edges with zero φ -curvature and “slope 45 degrees” are not absorbed (see Figure 6, left), and the evolution “cuts the vertices”. On the other hand, the edges with positive φ -curvature move with velocities

$$v_i^\varepsilon(t) = \frac{2}{\ell_i^\varepsilon(t)} + \frac{\alpha + \beta}{2} - \frac{(\beta - \alpha)\varepsilon}{4\ell_i^\varepsilon(t)}, \quad i = 1, 2.$$

Then, the effective evolution $E(t)$, in the limit $\varepsilon \rightarrow 0$, is given by the family of octagons whose moving edges have lengths $(\ell_1(t), \ell_2(t))$ solution to (19). Since the level set $\{U \leq 0\}$ is invariant under the flow of the ODEs system (19), $E(t)$ are octagons (not monotonically) converging to a stationary octagon as $t \rightarrow +\infty$ (see Figure 7).

If $U_0 = 0$, then in a time-lapse of order ε the evolution becomes a rectangle with the same features of the initial datum, but with $U_0^\varepsilon < 0$. Then the effective evolution is the one depicted above.

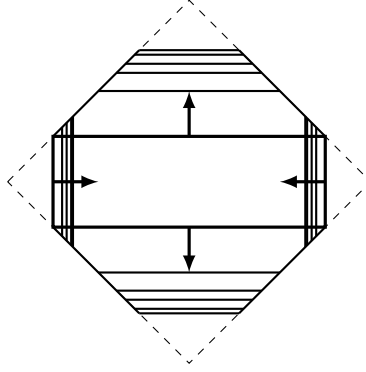


FIGURE 7. Effective evolutions, case 3 and $U_0 \leq 0$

If $U_0 > 0$, then the effective evolution maintains the rectangular shape for a short time (see Figure 8, left). Namely, the forced crystalline flow becomes a rectangle after a time lapse of order ε (see Figure 6), and then the geometric motion $E^\varepsilon(t)$ is given by “almost rectangles”, that is rectangles with small perturbations of order ε near the vertices, until the lengths of the edges with positive φ -curvature have velocities $v_2^\varepsilon(t) > -v_1^\varepsilon(t)$. Hence there exists $T > 0$ such that $E^\varepsilon(t)$ it can be approximated, in the Hausdorff topology and locally uniformly in $[0, T]$, by a family of rectangles $R(\ell_1^\varepsilon(t), \ell_2^\varepsilon(t))$ satisfying

$$\begin{cases} (\ell_1^\varepsilon)' = -2 \left(\frac{2}{\ell_2^\varepsilon} + \frac{\alpha + \beta}{2} - \frac{(\beta - \alpha)\varepsilon}{4\ell_2^\varepsilon} \right), \\ (\ell_2^\varepsilon)' = -2 \left(\frac{2}{\ell_1^\varepsilon} + \frac{\alpha + \beta}{2} - \frac{(\beta - \alpha)\varepsilon}{4\ell_1^\varepsilon} \right). \end{cases}$$

Passing to the limit as $\varepsilon \rightarrow 0$, we obtain a family of rectangles $E(t) = R(\ell_1(t), \ell_2(t))$, $t \in [0, T]$ where (ℓ_1, ℓ_2) is the solution of the system of ODEs (18) with initial datum in the set

$$A := \{U(\ell_1, \ell_2) > 0\} \cap \left\{ \ell_2 \leq \frac{-4}{\alpha + \beta} \leq \ell_1 \right\}.$$

Notice that the function

$$J(\ell_1, \ell_2) = 4(\log(\ell_2) - \log(\ell_1)) + (\alpha + \beta)(\ell_2 - \ell_1)$$

is a constant of motion for system (18). The phase portrait is shown in Figure 8. In particular, A is not a positively invariant set for the system, and the behavior of the trajectories depends on the energy level $J(\ell_{1,0}, \ell_{2,0})$ of the initial datum.

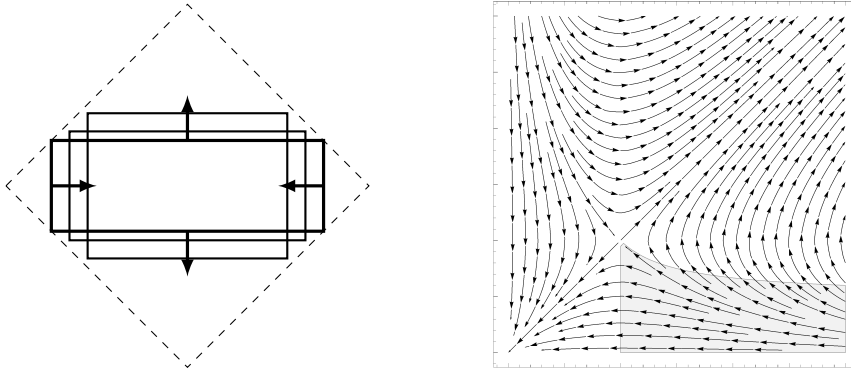


FIGURE 8. Left: short-time effective evolution, case 3 and $U_0 > 0$. Right: phase portrait of (18), with the region A .

The level set $\{J = 0\}$ is positively invariant in A , so that, if $J(\ell_{1,0}, \ell_{2,0}) = 0$, the effective evolution is given by rectangles converging, as $t \rightarrow +\infty$, to the equilibrium square $S(-4/(\alpha + \beta))$.

If $J(\ell_{1,0}, \ell_{2,0}) < 0$, then there exists a unique $t_0 > 0$ such that $\ell'_1(t_0) = -4/(\alpha + \beta)$, and the effective evolution for $t > t_0$ is the one shown in case (i): rectangles shrinking to a point in finite time.

If $J(\ell_{1,0}, \ell_{2,0}) > 0$, then the solution enters in the region $\{U \leq 0\}$ in finite time, so that the effective evolution becomes a family of octagons, converging to a stationary octagon in infinite time. \square

REFERENCES

- [1] F. Almgren and J.E. Taylor. Flat flow is motion by crystalline curvature for curves with crystalline energies. *J. Differential Geometry* **42** (1995), 1–22.
- [2] G. Barles, A. Cesaroni, M. Novaga. Homogenization of fronts in highly heterogeneous media. *SIAM J. Math. Anal.* **43** (2011), 212–227.
- [3] G. Bellettini, M. Novaga, M. Paolini. Characterization of facet breaking for nonsmooth mean curvature flow in the convex case. *Interfaces Free Bound.* **3** (2001), 415–446.
- [4] G. Bellettini, M. Novaga, M. Paolini. On a crystalline variational problem, part I: first variation and global L^∞ regularity. *Arch. Rational Mech. Anal.* **157** (2001), 165–191.
- [5] G. Bellettini, M. Novaga, M. Paolini. On a crystalline variational problem, part II: BV regularity and structure of minimizers on facets. *Arch. Rational Mech. Anal.* **157** (2001), 193–217.
- [6] A. Braides. *Γ -convergence for Beginners*. Oxford University Press, 2002.
- [7] A. Braides, *Local Minimization, Variational Evolution and Γ -convergence*. Lecture Notes in Mathematics, Springer, Berlin, 2014.
- [8] A. Braides, M. Cicalese, N. K. Yip. Crystalline Motion of Interfaces Between Patterns. *J. Stat. Phys.* **165** (2016), 274–319.

- [9] A. Braides, M.S. Gelli, M. Novaga. Motion and pinning of discrete interfaces. *Arch. Ration. Mech. Anal.* **95** (2010), 469–498.
- [10] A. Braides, A. Malusa, M. Novaga. Crystalline evolutions with rapidly oscillating forcing terms. Preprint arXiv:1707.03342 (2017).
- [11] A. Braides, G. Scilla. Motion of discrete interfaces in periodic media. *Interfaces Free Bound.* **15** (2013), 451–476.
- [12] A. Braides, M. Solci. Motion of discrete interfaces through mushy layers. *J. Nonlinear Sci.* **26** (2016), 1031–1053.
- [13] J. Cortes Discontinuous Dynamical Systems: A tutorial on solutions, nonsmooth analysis, and stability. *IEEE Control Systems Magazine* **28** (2008), 36–73.
- [14] A. Cesaroni, N. Dirr, M. Novaga. Homogenization of a semilinear heat equation. *J. Éc. polytech. Math.* **4** (2017), 633–660.
- [15] A. Cesaroni, M. Novaga, E. Valdinoci. Curve shortening flow in heterogeneous media. *Interfaces and Free Bound.* **13** (2011), 485–505.
- [16] A. Chambolle, M. Morini, M. Ponsiglione. Existence and uniqueness for a crystalline mean curvature flow. *Comm. Pure Appl. Math.*, to appear.
- [17] A. Chambolle, M. Morini, M. Novaga, M. Ponsiglione. Existence and uniqueness for anisotropic and crystalline mean curvature flows. Preprint arXiv:1702.03094 (2017).
- [18] A. Chambolle, M. Novaga. Approximation of the anisotropic mean curvature flow. *Math. Models Methods Appl. Sci.* **17** (2007), 833–844.
- [19] A. F. Filippov. *Differential Equations with Discontinuous Righthand Sides*, vol. 18 of Mathematics and Its Applications. Dordrecht, The Netherlands, Kluwer Academic Publishers, 1988.
- [20] Y. Giga. *Surface evolution equations. A level set approach*, vol. 99 of Monographs in Mathematics. Birkhäuser Verlag, Basel, 2006.
- [21] Y. Giga, M.E. Gurtin. A comparison theorem for crystalline evolution in the plane. *Quarterly of Applied Mathematics* **54** (1996), 727–737.
- [22] Y. Giga, P. Rybka. Facet bending in the driven crystalline curvature flow in the plane. *J. Geom. Anal.* **18** (2008), 109–147.
- [23] Y. Giga, P. Rybka. Facet bending driven by the planar crystalline curvature with a generic nonuniform forcing term. *J. Differential Equations* **246** (2009), 2264–2303.
- [24] M.E. Gurtin. *Thermomechanics of evolving phase boundaries in the plane*. Oxford Mathematical Monographs. The Clarendon Press, Oxford University Press, New York, 1993.
- [25] M. Novaga, E. Valdinoci. Closed curves of prescribed curvature and a pinning effect. *Netw. Heterog. Media* **6** (2011), no. 1, 77–88.
- [26] J.E. Taylor. Crystalline variational problems. *Bull. Amer. Math. Soc.* **84** (1978), 568–588.
- [27] J.E. Taylor, J. Cahn, C. Handwerker. Geometric Models of Crystal Growth. *Acta Metall. Mater.* **40** (1992), 1443–1474.